Journal of Organometallic Chemistry 695 (2010) 1375–1382

Contents lists available at ScienceDirect

Journal of Organometallic Chemistry

journal homepage: www.elsevier.com/locate/jorganchem

Syntheses and characterization of mono and dinuclear complexes of platinum group metals bearing benzene-linked bis(pyrazolyl)methane ligands

Kota Thirumala Prasad [a], Bruno Therrein [b], Kollipara Mohan Rao [a,*]

[a] Department of Chemistry, North Eastern Hill University, Shillong 793 022, India
[b] Service Analytique Facultaire, University of Neuchatel, Case Postale 158, CH-2009, Neuchatel, Switzerland

ARTICLE INFO

Article history:
Received 15 December 2009
Received in revised form 3 February 2010
Accepted 5 February 2010
Available online 13 February 2010

Keywords:
Arene-ligands
Bis(pyrazolyl)methane
Ruthenium
Rhodium
Iridium

ABSTRACT

Reaction of the benzene-linked bis(pyrazolyl)methane ligands, 1,4-bis{bis(pyrazolyl)-methyl}benzene (L1) and 1,4-bis{bis(3-methylpyrazolyl)methyl}benzene (L2), with pentamethylcyclopentadienyl rhodium and iridium complexes $[(\eta^5\text{-}C_5Me_5)M(\mu\text{-}Cl)Cl]_2$ (M = Rh and Ir) in the presence of NH_4PF_6 results under stoichiometric control in both, mono and dinuclear complexes, $[(\eta^5\text{-}C_5Me_5)RhCl(L)]^+$ {L = L1 (**1**); L2 (**2**)}, $[(\eta^5\text{-}C_5Me_5)IrCl(L)]^+$ {L = L1 (**3**); L2 (**4**)} and $[\{(\eta^5\text{-}C_5Me_5)RhCl\}_2(\mu\text{-}L)]^{2+}$ {L = L1 (**5**); L2 (**6**)}, $[\{(\eta^5\text{-}C_5Me_5)IrCl\}_2(\mu\text{-}L)]^{2+}$ {L = L1 (**7**); L2 (**8**)}. In contrast, reaction of arene ruthenium complexes $[(\eta^6$Ùarene)$Ru(\mu\text{-}Cl)Cl]_2$ (arene = C_6H_6, *p*-^{i}PrC_6H_4Me and C_6Me_6) with the same ligands (L1 or L2) gives only the dinuclear complexes $[\{(\eta^6\text{-}C_6H_6)RuCl\}_2(\mu\text{-}L)]^{2+}$ {L = L1 (**9**); L2 (**10**)}, $[\{(\eta^6\text{-}p\text{-}^i PrC_6H_4Me)RuCl\}_2(\mu\text{-}L)]^{2+}$ {L = L1 (**11**); L2 (**12**)} and $[\{(\eta^6\text{-}C_6Me_6)RuCl\}_2(\mu\text{-}L)]^{2+}$ {L = L1 (**13**); L2 (**14**)}. All complexes were isolated as their hexafluorophosphate salts. The single-crystal X-ray crystal structure analyses of [**7**]$(PF_6)_2$, [**9**]$(PF_6)_2$ and [**11**]$(PF_6)_2$ reveal a typical piano-stool geometry around the metal centers with six-membered metallo-cycle in which the 1,4-bis{bis(pyrazolyl)-methyl}benzene acts as a bis-bidentate chelating ligand.

1. Introduction

The coordination chemistry of poly(pyrazolyl)borate and methane ligands has revealed an impressive number of compounds with interesting structural, catalytic, and electronic properties [1–6]. The chemistry of poly(pyrazolyl)methane ligands is less extensive than that of their borate analogues due to the fact that convenient synthetic routes of functionalized neutral methane species have only recently been developed [7–10]. By functionalizing the pyrazolyl groups in the original poly(pyrazolyl)borate and -methane compounds, a multitude of "second-generation" ligands have been prepared [1–6]. More recently, functionalization of the borate or methane backbone has yielded a variety of "third-generation" ligands [11] as bis- and tris(pyrazolyl)methane compounds where two or more of the methane units are linked through organic spacers of varying degrees of flexibility, resulting in multitopic ligands.

The chemistry of "second generation" bis(pyrazolyl)methane complexes of rhodium, iridium and ruthenium is relatively less studied as compared to borate complexes of rhodium and iridium [11–13]. Indeed, the chemistry of arene ruthenium and pentamethylcyclopentadienyl (Cp*) rhodium and iridium complexes of bis(pyrazolyl)methane ligands bridged by a benzene-linker (third-generation) has yet to be explored. Arene ruthenium, rhodium and iridium complexes of bis(pyrazolyl)methanes have attracted attention due to their catalytic ability in reactions such as the alcoholysis of ketones and silanes, hydroformylation and hydroaminomethylation of alkenes and hydroamination [14–16]. Besides these, nitrogen donor ligands with platinum group metals have been shown to be effective catalysts for oxidation reactions [17] and for ring-opening metathesis polymerization [18] and recent studies of arene ruthenium complexes have shown that they are found to inhibit cancer cell growth [19,20].

In recent years, we have been carrying out arene ruthenium and Cp* rhodium and iridium complexation reactions with a variety of nitrogen-based ligands [21–27] including pyrazolyl-pyrimidine, pyrazolyl-pyridazine and pyridyl-pyridazine ligands. All of these ligands after coordination with metal have given five membered chelating complexes; this is the first time that isolated six-membered chelating complexes with 1,4-bis{bis(pyrazolyl)-methyl}benzene (L1) or 1,4-bis{bis(3-methylpyrazolyl)methyl}benzene (L2) (Chart 1) ligands have been isolated with these metal complexes.

In the present paper, we have synthesized homogeneous and immobilized half-sandwich rhodium, iridium and ruthenium complexes bearing bis(pyrazolyl)methanes bridged by benzene-linker, as bidentate or tetradentate bridging ligands (L). The Cp* rhodium and iridium complexes with ligands L give both mono and dinuclear complexes, while only dinuclear complexes are obtained with

* Corresponding author. Tel.: +91 364 272 2620; fax: +91 364 272 1010.
E-mail address: mohanrao59@gmail.com (K.M. Rao).

0022-328X/$ - see front matter © 2010 Elsevier B.V. All rights reserved.
doi:10.1016/j.jorganchem.2010.02.005

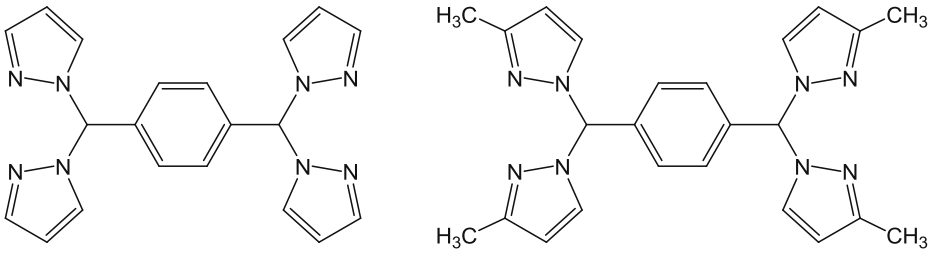

Chart 1.

arene ruthenium complexes. All these complexes are characterized by IR, NMR, mass spectrometry and UV–Vis spectroscopy. The molecular structures of three representative complexes are presented as well.

2. Experimental

2.1. General remarks

All reagents were purchased either from Aldrich or Fluka and used as received. All the experiments were performed under normal conditions. The ligands 1,4-bis{bis(pyrazolyl)-methyl}benzene (L1) and 1,4-bis{bis(3-methylpyrazolyl)methyl}benzene (L2), were synthesized by reported procedure [28] The dinuclear complexes $[(\eta^6\text{-}C_6H_6)Ru(\mu\text{-}Cl)Cl]_2$, $[(\eta^6\text{-}p\text{-}^iPrC_6H_4Me)Ru(\mu\text{-}Cl)Cl]_2$ and $[(\eta^6\text{-}C_6H_6)Ru(\mu\text{-}Cl)Cl]_2$ [29–31], and $[(\eta^5\text{-}C_5Me_5)M(\mu\text{-}Cl)Cl]_2$ (M = Rh and Ir) [32–34], were prepared according to literature methods. NMR spectra were recorded on Bruker AMX-400 MHz spectrometer. Infrared spectra were recorded as KBr pellets on a Perkin–Elmer 983 spectrophotometer. Elemental analyses were performed on a Perkin–Elmer-2400 CHN/S analyzer. Mass spectra were obtained from Waters ZQ-4000 mass spectrometer by ESI method. Absorption spectra were obtained at room temperature using a Perkin–Elmer Lambda 25 UV–Vis spectrophotometer.

2.2. General procedure for the syntheses of the mononuclear complexes **1**–**4**

A mixture of $[(\eta^5\text{-}C_5Me_5)M(\mu\text{-}Cl)Cl]_2$ (M = Rh, Ir) (0.08 mmol), ligand L (L1 or L2) (0.17 mmol) and 2.5 equiv of NH_4PF_6 in dry methanol (20 ml) was refluxed at 50 °C for 6–8 h, after which an orange precipitate was observed. The precipitate was separated by filtration, washed with cold methanol, diethyl ether and dried in vacuo.

2.2.1. $[(\eta^5\text{-}C_5Me_5)Rh(L1)Cl]PF_6$ ([**1**]PF_6)

Yield: 90 mg (72%). ^{1}H NMR (400 MHz, CD_3CN) δ = 8.29 (s, 1H, $CH(pz)_2$), 8.05 (d, 2H, J = 1.80 Hz, pz-5H), 7.91 (d, 2H, J = 2.40 Hz, pz-3H), 7.78 (s, 1H, $CH(pz)_2$), 7.64 (d, 2H, J = 1.2 Hz, pz-5H), 7.58 (d, 2H, J = 2.40 Hz, pz-3H), 7.05 (d, 2H, J = 7.2 Hz, C_6H_4), 6.75 (d, 2H, J = 6.8 Hz, C_6H_4), 6.41–6.38 (m, 4H, pz-4H), 1.54 (s, 15H, C_5Me_5); IR (KBr, cm^{-1}): 3441(w), 3134(m), 1629(m), 1447(m), 1399(m), 1296(m), 1103(m), 845(s), 760(m), 558(m); ESI-MS: 643.8 [M^+], 608.5 [M−Cl]; UV–Vis {acetonitrile, λ_{max} nm (ε 10^{-5} M^{-1} cm^{-1})}: 223 (0.59), 341 (0.04); Anal. Calc. for $C_{30}H_{33}F_6N_8PRhCl$ (788.9): C, 45.67; H, 4.22; N 14.20. Found: C, 45.53; H, 4.23; N, 14.13%.

2.2.2. $[(\eta^5\text{-}C_5Me_5)Rh(L2)Cl]PF_6$ ([**2**]PF_6)

Yield 99 mg (74%). ^{1}H NMR (400 MHz, CD_3CN) δ = 8.31 (s, 1H, $CH(pz)_2$), 8.01 (d, 2H, J = 1.80 Hz, pz-5H), 7.81 (s, 1H, $CH(pz)_2$), 7.62 (d, 2H, J = 1.2 Hz, pz-5H), 7.07 (d, 2H, J = 7.2 Hz, C_6H_4), 6.76 (d, 2H, J = 6.8 Hz, C_6H_4), 6.41–6.37 (m, 4H, pz-4H), 2.61 (bs, 6H, Pz-3Me), 2.38 (bs, 6H, Pz-3Me), 1.58 (s, 15H, C_5Me_5); IR (KBr, cm^{-1}): 3441(w), 3134(m), 1629(m), 1447(m), 1399(m), 1296(m), 1103(m), 845(s), 760(m), 558(m); ESI-MS: 700.6 [M^+], 675.6 [M−Cl]; UV–Vis {acetonitrile, λ_{max} nm (ε 10^{-5} M^{-1} cm^{-1})}: 229 (0.43), 394 (0.22); Anal. Calc. for $C_{34}H_{41}F_6RhN_8PCl$ (845.6): C, 48.32; H, 4.89; N, 13.26. Found: C, 48.23; H, 4.91; N, 13.18%.

2.2.3. $[(\eta^5\text{-}C_5Me_5)Ir(L1)Cl]PF_6$ ([**3**]PF_6)

Yield: 90 mg (64%). ^{1}H NMR (400 MHz, CD_3CN) δ = 8.26 (s, 1H, $CH(pz)_2$), 7.99 (d, 2H, J = 1.80 Hz, pz-5H), 7.87 (d, 2H, J = 2.40 Hz, pz-3H), 7.78 (s, 1H, $CH(pz)_2$), 7.61 (d, 2H, J = 1.2 Hz, pz-5H), 7.50 (d, 2H, J = 2.40 Hz, pz-3H), 7.05 (d, 2H, J = 7.2 Hz, C_6H_4), 6.75 (d, 2H, J = 6.8 Hz, C_6H_4), 6.39–6.36 (m, 4H, pz-4H), 1.52 (s, 15H, C_5Me_5); IR (KBr, cm^{-1}): 3448(w), 3134(m), 1627(m), 1446(m), 1399(m), 1296(m), 1103(m), 843(s), 760(m), 558(m); ESI-MS: 733.3 [M^+], 698.1 [M−Cl]; UV–Vis {acetonitrile, λ_{max} nm (ε 10^{-5} M^{-1} cm^{-1})}: 225(0.73), 352 (0.038); Anal. Calc. for $C_{30}H_{33}F_6N_8PIrCl$ (878.5): C, 41.03; H, 3.79; N, 12.76. Found: C, 43.93; H, 3.73; N, 12.65%.

2.2.4. $[(\eta^5\text{-}C_5Me_5)Ir(L2)Cl]PF_6$ ([**4**]PF_6)

Yield 89 mg (60%). ^{1}H NMR (400 MHz, CD_3CN) δ = 8.27 (s, 1H, $CH(pz)_2$), 8.02 (d, 2H, J = 1.80 Hz, pz-5H), 7.76 (s, 1H, $CH(pz)_2$), 7.62 (d, 2H, J = 1.2 Hz, pz-5H), 7.09 (d, 2H, J = 7.2 Hz. C_6H_4), 6.78 (d, 2H, J = 6.8 Hz, C_6H_4), 6.42–6.36 (m, 4H, pz-4H), 2.63 (s, 6H, Pz-3Me), 2.37 (s, 6H, Me_3-Pz), 1.55 (s, 15H, C_5Me_5); IR (KBr, cm^{-1}): 3441(w), 3134(m), 1629(m), 1447(m), 1399(m), 1296(m), 1103(m), 845(s), 760(m), 558(m); ESI-MS: 789.4 [M^+], 754.2 [M−Cl]; UV–Vis {acetonitrile, λ_{max} nm (ε 10^{-5} M^{-1} cm^{-1})}: 228 (0.51), 485 (0.02); Anal. Calc. for $C_{34}H_{41}F_6IrN_8PCl$ (934.8): C, 43.70; H, 4.42; N, 11.99. Found: C, 43.67; H, 4.49; N, 11.86%.

2.3. General procedure for the syntheses of the dinuclear complexes **5**–**8**

A mixture of $[(Cp^*)M(\mu\text{-}Cl)Cl]_2$ (M = Rh, Ir) (0.08 mmol), ligand L (L1 or L2) (0.08 mmol) and 2.5 equiv of NH_4PF_6 in dry methanol (20 ml) was refluxed at 50 °C for 12 h, after which a dark orange precipitate was formed. The precipitate was separated by filtration, washed with cold methanol, diethyl ether and dried in vacuo.

2.3.1. $[\{(\eta^5\text{-}C_5Me_5)RhCl\}_2(\mu\text{-}L1)](PF_6)_2$ ([**5**]$(PF_6)_2$)

Yield 80 mg (84%). ^{1}H NMR (400 MHz, CD_3CN) δ = 8.31 (s, 2H, $CH(pz)_2$), 8.09 (d, 4H, J = 1.60 Hz, pz-5H), 7.95 (d, 4H, J = 2.11 Hz, pz-3H), 6.76 (s, 4H, C_6H_4), 6.41 (dd, 4H, J = 1.20 Hz, pz-4H), 1.48 (s, 30H, C_5Me_5); IR (KBr, cm^{-1}): 3446(w), 3134(m), 1629(m), 1446(m), 1401(m), 1295(m), 1103(m), 843(s), 760(m), 555(m); ESI-MS: 1062.6 [M^{2+}+PF_6^-]$^+$; UV–Vis {acetonitrile, λ_{max} nm (ε 10^{-5} M^{-1} cm^{-1})}: 224 (0.54), 307 (0.05) and 437 (0.01); Anal. Calc. for $C_{40}H_{48}F_{12}N_8P_2Rh_2Cl_2$ (1207.6): C, 39.79; H, 4.01; N, 9.28. Found: C, 39.53; H, 4.06; N, 9.19%.

2.3.2. [{(η^5-Cp)RhCl}$_2$(μ-L2)](PF$_6$)$_2$ ([**6**](PF$_6$)$_2$)*

Yield 80 mg (84%). ^{1}H NMR (400 MHz, CD_3CN) 8.33 (s, 2H, CH(pz)$_2$), 8.07 (d, 4H, *J* = 1.64 Hz, pz-5H), 6.78 (s, 4H, C_6H_4), 6.39 (dd, 4H, *J* = 1.20 Hz, pz-4H), 2.76 (s, 12H, pz-3Me), 1.49 (s, 30H, C_5Me_5); IR (KBr, cm^{-1}): 3446(b), 3131(m), 1627(m), 1446(m), 1408(m), 1296(m), 1103(m), 845(s), 761(m), 585(m); ESI-MS: 1118.6 [M^{2+}+PF_6^-]$^+$; UV–Vis {acetonitrile, λ_{max} nm (ε 10^{-5} M^{-1} cm^{-1})}: 228 (0.59), 310 (0.04) and 430 (0.02); Anal. Calc. for $C_{44}H_{56}Cl_2F_{12}N_4P_2Rh_2$ (1263.6): C, 41.82; H, 4.47; N, 8.87. Found: C, 41.71; H, 4.55; N, 8.65%.

*2.3.3. [{(η^5-C_5Me_5)IrCl}$_2$(μ-L1)](PF$_6$)$_2$ ([**7**](PF$_6$)$_2$)*

Yield 91 mg (77%). ^{1}H NMR (400 MHz, CD_3CN) δ = 8.32 (s, 2H, CH(pz)$_2$), 8.06 (d, 4H, *J* = 1.62 Hz, pz-5H), 8.01 (d, 4H, *J* = 2.16 Hz, pz-3H), 6.78 (s, 4H, C_6H_4), 6.44 (dd, 4H, *J* = 1.22 Hz, pz-4H), 1.51 (s, 30H, C_5Me_5); IR (KBr, cm^{-1}): 3441(b), 3134(m), 1629(m), 1447(m), 1399(m), 1296(m), 1103(m), 845(s), 760(m), 558(m); ESI-MS: 1241.5 [M^{2+}+PF_6^-]$^+$; UV–Vis {acetonitrile, λ_{max} nm (ε 10^{-5} M^{-1} cm^{-1})}: 225 (0.58), 312 (0.04) and 391 (0.03); Anal. Calc. for $C_{40}H_{48}Cl_2F_{12}Ir_2N_8P_2$ (1386.2): C, 34.66; H, 3.49; N, 8.08. Found: C, 34.42; H, 3.52; N, 8.01%.

*2.3.4. [{(η^5-C_5Me_5)IrCl}$_2$(μ-L2)](PF$_6$)$_2$ ([**8**](PF$_6$)$_2$)*

Yield 81 mg (65%). ^{1}H NMR (400 MHz, CD_3CN) δ = 8.33 (s, 2H, CH(pz)$_2$), 8.09 (d, 4H, *J* = 1.60 Hz, pz-5H), 6.74 (s, 4H, C_6H_4), 6.44 (dd, 4H, *J* = 1.20 Hz, pz-4H), 2.76–2.80 (s, 12H, pz-3Me), 1.48 (s, 30H, C_5Me_5); IR (KBr, cm^{-1}): 3446(b), 3134(m), 1629(m), 1446(m), 1401(m), 1295(m), 1103(m), 843(s), 760(m), 558(m); ESI-MS: 1297.5 [M^{2+}+PF_6^-]$^+$; UV–Vis {acetonitrile, λ_{max} nm (ε 10^{-5} M^{-1} cm^{-1})}: 228 (0.71), 316 (0.04) and 397 (0.02); Anal. Calc. for $C_{44}H_{56}Cl_2F_{12}Ir_2N_8P_2$ (1442.2): C, 36.64; H, 3.91; N, 7.77. Found: C, 36.62; H, 3.99; N, 7.65%.

*2.4. General procedure for the synthesis of the dinuclear complexes **9**–**14***

A mixture of [(η^6-arene)Ru(μ-Cl)Cl]$_2$ (arene = C_6H_6, *p*-^{i}PrC_6H_4Me or C_6Me_6) (0.1 mmol), ligand L (L1 or L2) (0.1 mmol) and 2.5 equiv of NH_4PF_6 in dry methanol (15 ml) was stirred at room temperature for 10 h, after which an orange precipitate was observed. The precipitate was filtered, washed with cold methanol, diethyl ether and dried in vacuo.

*2.4.1. [{(η^6-C_6H_6)RuCl}$_2$(μ-L1)](PF$_6$)$_2$ ([**9**](PF$_6$)$_2$)*

Yield 80 mg (72%). ^{1}H NMR (400 MHz, CD_3CN) δ = 8.26 (s, 2H, CH(pz)$_2$), 8.07 (d, 4H, *J* = 1.40 Hz, pz-5H), 7.95 (d, 4H, *J* = 2.00 Hz, pz-3H), 6.75 (s, 4H, C_6H_4), 6.41 (dd, 4H, *J* = 1.24 Hz, pz-4H), 5.40 (s, 12H, C_6H_6); IR (KBr, cm^{-1}): 3441(b), 3134(m), 1629(m), 1447(m), 1399(m), 1296(m), 1103(m), 845(s), 760(m), 558(m); ESI-MS: 944.8 [M^{2+}+PF_6^-]$^+$; UV–Vis {acetonitrile, λ_{max} nm (ε 10^{-5} M^{-1} cm^{-1})}: 226 (0.73), 307 (0.05) and 428 (0.01); Anal. Calc. for $C_{32}H_{30}Cl_2F_{12}N_8P_2Ru_2$ (1089.6): C, 35.27; H, 2.78; N, 10.28. Found: C, 35.15; H, 2.81; N, 10.18%.

*2.4.2. [{(η^6-C_6H_6)RuCl}$_2$(μ-L2)](PF$_6$)$_2$ ([**10**](PF$_6$)$_2$)*

Yield 76 mg (66%). ^{1}H NMR (400 MHz, CD_3CN) δ = 8.31 (s, 2H, CH(pz)$_2$), 8.07 (d, 4H, *J* = 1.40 Hz, pz-5H), 6.78 (s, 4H, C_6H_4), 6.46 (dd, 4H, *J* = 1.24 Hz, pz-4H), 5.48 (s, 12H, C_6H_6), 2.86 (s, 12H, pz-3Me); IR (KBr, cm^{-1}): 3448(b), 3134(m), 1627(m), 1446(m), 1399(m), 1296(m), 1103(m), 843(s), 760(m), 558(m); ESI-MS: 1000.2 [M^{2+}+PF_6^-]$^+$; UV–Vis {acetonitrile, λ_{max} nm (ε 10^{-5} M^{-1} cm^{-1})}: 229 (0.65), 316 (0.05) and 430 (0.02); Anal. Calc. for $C_{36}H_{38}Cl_2F_{12}N_8P_2Ru_2$ (1145.7): C, 37.74; H, 3.34; N, 9.78. Found: C, 37.65; H, 3.35; N, 9.65%.

*2.4.3. [{(η^6-*p*-^{i}PrC_6H_4Me)RuCl}$_2$(μ-L1)](PF$_6$)$_2$ ([**11**](PF$_6$)$_2$)*

Yield 91 mg (81%). ^{1}H NMR (400 MHz, CD_3CN) δ = 8.32 (s, 2H, CH(pz)$_2$), 8.04 (d, 4H, *J* = 1.40 Hz, pz-5H), 7.95 (d, 4H, *J* = 2.04 Hz, pz-3H), 6.76 (s, 4H, C_6H_4), 6.41 (dd, 4H, *J* = 1.28 Hz, pz-4H), 5.57 (d, 4H, *J* = 5.60 Hz, $Ar_{p\text{-}cy}$), 5.38 (d, 4H, *J* = 5.80 Hz, $Ar_{p\text{-}cy}$), 2.84 (sept, 2H, CH(CH$_3$)$_2$), 2.17 (s, 6H, $Ar_{p\text{-}cy}$-Me), 1.25 (d, 6H, CH(CH$_3$)$_2$); 1.21 (d, 6H, CH(CH$_3$)$_2$); IR (KBr, cm^{-1}): 3441(b), 3134(m), 1629(m), 1447(m), 1399(m), 1296(m), 1103(m), 845(s), 760(m), 558(m); ESI-MS: 1056.2 [M^{2+}+PF_6^-]$^+$; UV–Vis {acetonitrile, λ_{max} nm (ε 10^{-5} M^{-1} cm^{-1})}: 224 (0.65), 316 (0.05) and 431 (0.02); Anal. Calc. for $C_{40}H_{46}Cl_2F_{12}N_8P_2Ru_2$ (1201.8): C, 39.97; H, 3.86; N, 9.32. Found: C, 39.78; H, 3.97; N, 9.27%.

*2.4.4. [{(η^6-*p*-^{i}PrC_6H_4Me)RuCl}$_2$(μ-L2)](PF$_6$)$_2$ ([**12**](PF$_6$)$_2$)*

Yield 79 mg (63%). ^{1}H NMR (400 MHz, CD_3CN) δ = 8.34 (s, 2H, CH(pz)$_2$), 8.03 (d, 4H, *J* = 1.40 Hz, pz-5H), 6.76 (s, 4H, C_6H_4), 6.41 (d, 4H, *J* = 3.20 Hz, pz-4H), 5.55 (d, 4H, *J* = 5.60 Hz, $Ar_{p\text{-}cy}$), 5.39 (d, 4H, *J* = 5.80 Hz, $Ar_{p\text{-}cy}$), 2.87 (s, 12H, pz-3Me), 2.79 (sept, 2H, CH(CH$_3$)$_2$), 2.16 (s, 6H, $Ar_{p\text{-}cy}$-Me), 1.26 (d, 6H, CH(CH$_3$)$_2$); 1.21 (d, 6H, CH(CH$_3$)$_2$); IR (KBr, cm^{-1}): 3446(b), 3134(m), 1627(m), 1448(m), 1399(m), 1296(m), 1105(m), 843(s), 762(m), 558(m); ESI-MS: 1112.2 [M^{2+}+PF_6^-]$^+$; UV–Vis {acetonitrile, λ_{max} nm (ε 10^{-5} M^{-1} cm^{-1})}: 229 (0.56), 307 (0.05) and 437 (0.02); Anal. Calc. for $C_{44}H_{54}Cl_2F_{12}N_4P_2Ru_2$ (1257.9): C, 42.01; H, 4.33; N, 8.91. Found: C, 41.93; H, 4.36; N, 8.87%.

*2.4.5. [{(η^6-C_6Me_6)RuCl}$_2$(μ-L1)](PF$_6$)$_2$ ([**13**](PF$_6$)$_2$)*

Yield 101 mg (80%). ^{1}H NMR (400 MHz, CD_3CN) δ = 8.35 (s, 2H, CH(pz)$_2$), 8.07 (d, 4H, *J* = 1.40 Hz, pz-5H), 7.97 (d, 4H, *J* = 2.00 Hz, pz-3H), 6.75 (s, 4H, C_6H_4), 6.44 (dd, 4H, *J* = 1.24 Hz, pz-4H), 2.28 (s, 36H, C_6Me_6); IR (KBr, cm^{-1}): 3441(b), 3134(m), 1629(m), 1447(m), 1399(m), 1296(m), 1103(m), 845(s), 760(m), 558(m); ESI-MS: 1112.8 [M^{2+}+PF_6^-]$^+$; UV–Vis {acetonitrile, λ_{max} nm (ε 10^{-5} M^{-1} cm^{-1})}: 228 (0.68), 312 (0.05) and 427 (0.02); Anal. Calc. for $C_{44}H_{54}Cl_2F_{12}N_8P_2Ru_2$ (1257.9): C, 42.01; H, 4.33; N, 8.91. Found: C, 42.05; H, 4.41; N, 8.88%.

*2.4.6. [{(η^6-C_6Me_6)RuCl}$_2$(μ-L2)](PF$_6$)$_2$ ([**14**](PF$_6$)$_2$)*

Yield 86 mg (65%). ^{1}H NMR (400 MHz, CD_3CN) δ = 8.36 (s, 2H, CH(pz)$_2$), 8.07 (d, 4H, *J* = 1.40 Hz, pz-5H), 6.78 (s, 4H, C_6H_4), 6.46 (d, 4H, *J* = 2.24 Hz, pz-4H), 2.85 (s, 12H, pz-3Me), 2.26 (s, 36H, C_6Me_6); IR (KBr, cm^{-1}): 3446(b), 3135(m), 1626(m), 1446(m), 1402(m), 1296(m), 1103(m), 844(s), 760(m), 558(m); ESI-MS: 1169.8 [M^{2+}+PF_6^-]$^+$; UV–Vis {acetonitrile, λ_{max} nm (ε 10^{-5} M^{-1} cm^{-1})}: 229 (0.71), 317 (0.04) and 397 (0.03); Anal. Calc. for $C_{48}H_{62}Cl_2F_{12}N_8P_2Ru_2$ (1314.1): C, 43.87; H, 4.76; N, 8.53. Found: C, 43.75; H, 4.75; N, 8.52%.

2.5. Single-crystal X-ray structure analyses

Crystals of complexes [**7**](PF$_6$)$_2$, [**9**](PF$_6$)$_2$ and [**11**](PF$_6$)$_2$ were mounted on a Stoe Image Plate Diffraction system equipped with a φ circle goniometer, using Mo-Kα graphite monochromated radiation (λ = 0.71073 Å) with φ range 0–200°. The structures were solved by direct methods using the program SHELXS–97 [35]. Refinement and all further calculations were carried out using SHELXL-97 [36]. The H-atoms were included in calculated positions and treated as riding atoms using the SHELXL default parameters. The non-H atoms were refined anisotropically, using weighted full-matrix least-square on F^2. In [**7**](PF$_6$)$_2$·2CH$_3$CN, the residual electron densities greater than 1 e Å^{-3} are all located at less than 1 Å from the iridium atoms. Crystallographic details are summarized in Table 1 and selected bond lengths and angles are presented in Table 2. Figs. 1–3 were drawn with ORTEP–32 [37].

Table 1
Crystallographic and structure refinement parameters for complexes [**7**]$(PF_6)_2{\cdot}2CH_3CN$, [**9**]$(PF_6)_2{\cdot}CH_3CN$ and [**11**]$(PF_6)_2{\cdot}2CH_3CN$.

	[**7**]$(PF_6)_2{\cdot}2CH_3CN$	[**9**]$(PF_6)_2{\cdot}CH_3CN$	[**11**]$(PF_6)_2{\cdot}2CH_3CN$
Chemical formula	$C_{44}H_{54}Cl_2F_{12}Ir_2N_{10}P_2$	$C_{34}H_{33}Cl_2F_{12}N_{10}P_2Ru_2$	$C_{44}H_{52}Cl_2F_{12}N_{10}P_2Ru_2$
Formula weight	1468.21	1130.67	1283.94
Crystal system	Monoclinic	Monoclinic	Monoclinic
Space group	$P2_1/n$ (no. 14)	$P2_1/n$ (no. 14)	$P2_1/c$ (no. 14)
Crystal color and shape	Orange block	Orange block	Orange block
Crystal size	0.27 × 0.24 × 0.22	0.25 × 0.22 × 0.18	0.23 × 0.19 × 0.15
a (Å)	13.6968(13)	15.3761(9)	9.4659(7)
b (Å)	14.0285(9)	13.9492(10)	25.737(2)
c (Å)	14.5963(14)	19.9223(13)	11.0998(9)
β (°)	114.169(10)	105.567(7)	110.868(9)
V (Å^3)	2558.8(4)	4116.3(5)	2526.8(3)
Z	2	4	2
T (K)	173(2)	173(2)	173(2)
D_{calc} (g cm^{-3})	1.906	1.824	1.688
μ (mm^{-1})	5.45	1.036	0.855
Scan range (°)	2.11 < θ < 26.18	2.09 < θ < 26.04	2.12 < θ < 26.04
Unique reflections	5045	8055	4849
Reflections used [$I > 2\sigma(I)$]	3675	4212	3295
R_{int}	0.0745	0.0944	0.0591
Final R indices [$I > 2\sigma(I)$][a]	0.0415, wR_2 0.1038	0.0428, wR_2 0.0789	0.0463, wR_2 0.1189
R indices (all data)	0.0616, wR_2 0.1103	0.0982, wR_2 0. 0872	0.0704, wR_2 0.1269
Goodness-of-fit	0.927	0.797	0.961
Max, Min $\Delta\rho$/e (Å^{-3})	3.086, −2.055	0.952, −0.929	1.538, −0.792

[a] Structures were refined on F_0^2 : $wR_2 = [\sum[w(F_0^2 - F_c^2)^2]/\sum w(F_0^2)^2]^{1/2}$, where $w^{-1} = [\sum(F_0^2) + (aP)^2 + bP]$ and $P = [\max(F_0^2, 0) + 2F_c^2]/3$.

Table 2
Selected bond lengths and angles for complexes [**7**]$(PF_6)_2{\cdot}2CH_3CN$, [**9**]$(PF_6)_2{\cdot}CH_3CN$ and [**11**]$(PF_6)_2{\cdot}2CH_3CN$.

	[**7**]$(PF_6)_2$	[**9**]$(PF_6)_2$	[**11**]$(PF_6)_2$
Inter atomic distances (Å)			
M–M	9.4781(9)	8.8236(8)	8.8285(13)
M–N1	2.110(6)	2.086(4)	2.102(4)
M–N3	2.093(6)	2.089(5)	2.098(4)
M–N5		2.081(4)	
M–N7		2.085(5)	
M–Cl1	2.394(2)	2.395(2)	2.391(1)
M–Cl2		2.392(2)	
M-centroid[a]	1.788	1.668	1.673
N1–N2	1.345(8)	1.352(6)	1.351(6)
N3–N4	1.372(8)	1.358(7)	1.350(6)
N5–N6		1.366(6)	
N7–N8		1.366(6)	
Angles (°)			
N1–M–N3	86.0(2)	84.31(17)	85.08(16)
N5–M–N7	83.82(17)		
N1–M–Cl1	84.01(17)	84.42(13)	85.20(11)
N3–M–Cl1	83.36(18)	84.80(13)	83.15(11)
N5–M–Cl2		84.54(12)	
N7–M–Cl2		84.77(13)	
M–N1–N2	125.4(5)	124.6(3)	126.2(3)
M–N3–N4	125.9(5)	125.4(3)	125.2(3)
M–N5–N6		125.4(3)	
M–N7–N8		125.5(3)	

[a] Calculated centroid-to-metal distances (η^6-C_6 or η^5-C_5 coordinated aromatic ring).

3. Results and discussion

3.1. Synthesis of the mononuclear complexes *1–4* as hexafluorophosphate salts

The mononuclear cationic pentamethylcyclopentadienyl rhodium and iridium complexes having 1,4-bis{bis(pyrazolyl)-methyl}benzene (L1) and 1,4-bis{bis(3-methylpyrazolyl)methyl}-benzene (L2) ligands *viz*., $[(\eta^5\text{-}C_5Me_5)RhCl(L)]^+$ {L = L1 (**1**), L2 (**2**)}, $[(\eta^5\text{-}C_5Me_5)IrCl(L)]^+$ {L = L1 (**3**), L2 (**4**)} (Scheme 1), have been prepared by the reaction of pentamethylcyclopentadienyl complexes $[(\eta^5\text{-}C_5Me_5)M(\mu\text{-}Cl)Cl]_2$ (M = Rh, Ir) with two equivalents of ligands L1 or L2 in methanol. These complexes are isolated as their hexafluorophosphate salts and complexes **1–4** are orange/red, non-hygroscopic, and air-stable, shiny crystalline solids. They are sparingly soluble in methanol, dichloromethane, chloroform and acetone, but well soluble in acetonitrile and dimethylsulphoxide.

3.2. Characterization of the mononuclear complexes *1–4*

All these mononuclear complexes were characterized by IR, ^{1}H NMR, mass and elemental analysis. The infrared spectra of the complexes **1–4** exhibit a strong band in the region 844–850 cm^{-1} for a typical ν_{P-F} stretching band and a medium band in the region 555–558 cm^{-1} δ_{P-F} for the PF_6 anion. Moreover, all complexes show absorption bands around 1620–1631, 1446–1458, 1270–1296 and 1103–1058 cm^{-1} corresponding to $\nu_{C=N}$ vibrations of pyrazoles [38,39]. Besides these absorptions, two absorption bands at 2990–3050 cm^{-1} and 3400–3450 cm^{-1} were also observed for N–H vibrations. The mass spectra of these complexes **1–4** exhibit the corresponding molecular ion peaks at m/z = 643, 700, 733 and 789.

The ^{1}H NMR spectra of free ligand (L1 or L2) exhibit a characteristic set of five resonances for the pyrazole, methyl and benzene ring protons. However the ^{1}H NMR spectrum of L2 ligand shown two types of isomers, they are 3 and 5-methyl substituted pyrazoles. From the proton NMR studies indicated the ratio of 3 and 5 isomers are 78% and 22%, respectively, since it was prepared from terphthaldehyde and 3-methyl-pyrazole [28]. Upon formation of the complexes with this ligand (L2), the detection of signals of 5 methyl isomer is not noticed in the NMR spectrum due to the domination of 3 methyl substituted pyrazole NMR signals. So the signal intensity of later isomer (5-methyl substituted pyrazole) is so small and difficult to assign methyl protons in all the complexes. The mononuclear cationic complexes **1–4** exhibit ten distinct resonances assignable to pyrazole or methyl-pyrazole and benzene ring protons of the (L1 or L2) ligand indicating formation of mononuclear complexes. The methylic proton {–C***H***(Pz)2–} of ligand has shown two singlets at δ = 8.29 and 7.78 corresponding to coordinated and uncoordinated to the metal complex indicating

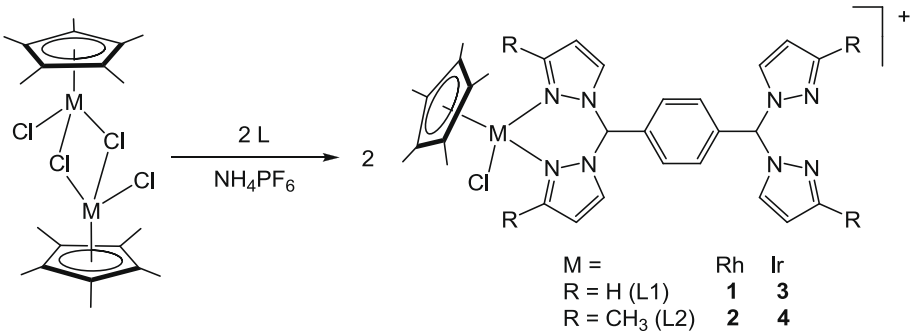

Scheme 1.

formation of mono nuclear compounds. Besides these resonances complexes **1**–**4** exhibit a singlet at $\delta \approx 1.5$ for the protons of the pentamethylcyclopentadienyl ligand.

3.3. Synthesis of dinuclear complexes *5*–*14* as hexafluorophosphate salts

The reaction of the chloro bridged dinuclear complexes $[(\eta^5\text{-}C_5Me_5)M(\mu\text{-}Cl)Cl]_2$ (M = Rh, Ir); $[(\eta^6\text{-arene})Ru(\mu\text{-}Cl)Cl]_2$ (arene = C_6H_6, *p*-^{i}PrC_6H_4Me and C_6Me_6) with 1 equiv of 1,4-bis{bis(pyrazolyl)-methyl}benzene (L1) or 1,4-bis{bis(3-methylpyrazolyl) methyl}-benzene (L2) in methanol results in the formation of orange, air-stable, dinuclear dicationic complexes $[\{(\eta^5\text{-}C_5Me_5)RhCl\}_2(\mu\text{-L})]^{2+}$ {L = L1 (**5**); Lp2 (**6**)}, $[\{(\eta^5\text{-}C_5Me_5)IrCl\}_2(\mu\text{-L})]^{2+}$ {L = L1 (**7**); L2 (**8**)}, $[\{(\eta^6\text{-}C_6H_6)RuCl\}_2(\mu\text{-L})]^{2+}$ {L = L1 (**9**); L2 (**10**)}, $[\{(\eta^6\text{-}p\text{-}^iPrC_6H_4Me)RuCl\}_2(\mu\text{-L})]^{2+}$ {L = L1 (**11**); L2 (**12**)} and $[\{(\eta^6\text{-}C_6H_6)RuCl\}_2(\mu\text{-L})]^{2+}$ {L = L1 (**13**); L2 (**14**)}. All complexes are isolated as their hexafluorophosphate salts (Scheme 2) and they are characterized by IR, mass, ^{1}H NMR spectrometry, UV–Vis spectroscopy, and elemental analysis.

3.4. Characterization of the dinuclear complexes *5*–*14*

Infrared spectra of the dinuclear complexes **5**–**14** show a similar trend as the mononuclear cationic complexes **1**–**4**. The mass spectra of the complexes **5**–**14** give rise to two main peaks; a minor peak with an approximately 50% intensity attributed to $[M^{2+}+PF_6^-]^+$ at *m/z* 1062, 1118, 1241, 1297, 944, 1000, 1056, 1112, 1112 and 1169, respectively, and a major peak, which corresponds to loss of $[(Cp^*/arene)MCl]^+$ fragment and the formation of mononuclear cations **1**–**6** at *m/z* = 643, 700, 733, 789, 585, 641, 641, 697, 669 and 725, respectively.

The ^{1}H NMR spectra of the dinuclear dicationic complexes **5**–**14** exhibited five distinct resonances assignable to pyrazole rings, methyl and benzene ring protons of the ligands (L1 or L2) indicating formation of dinuclear complexes. The methylic proton {–C***H***(Pz)2–} of ligand has exhibited a singlet at δ = 8.36–8.33 indicating formation of dinuclear compounds. Besides these resonances complexes **5**–**8** exhibit a singlet at $\delta \approx 1.5$ for the protons of the pentamethylcyclopentadienyl ligands. Interestingly, in these complexes the chemical shift of the protons of the pentamethylcyclopentadienyl ligands does not show downfield shift as like with

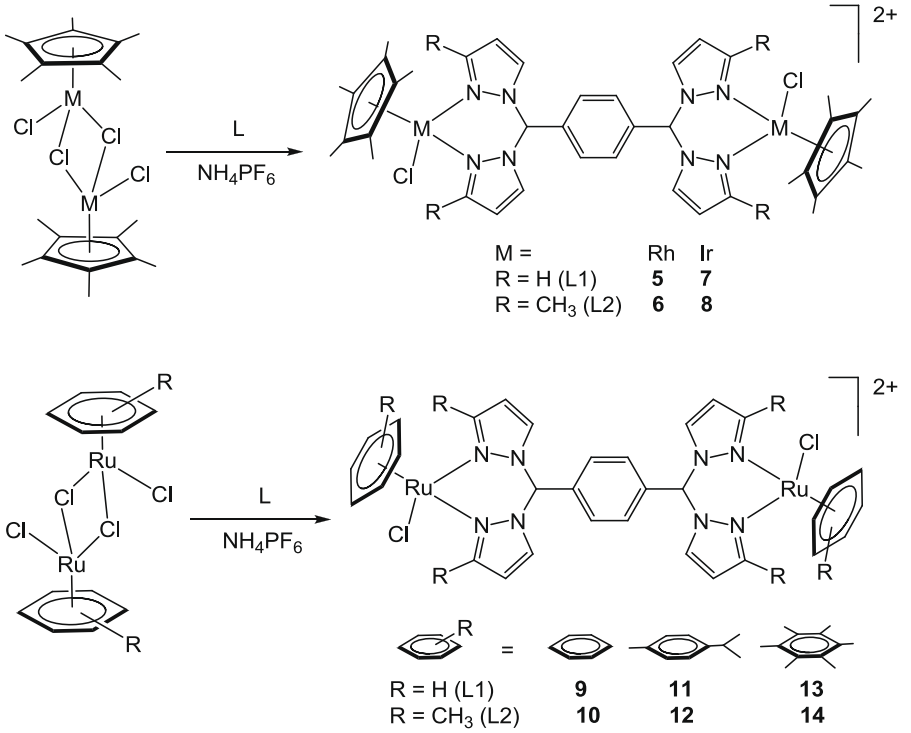

Scheme 2.

other nitrogen-based ligands [21–27]. Complexes **9** and **10** exhibit a singlet at $\delta = 5.40$ and 5.48 for protons of benzene ligands, complexes **11** and **12** exhibits a doublet at $\delta = 1.21$ for the protons of the isopropyl methyl groups, a singlet at $\delta = 1.26$ for the methyl protons, a septet at $\delta = 2.79$ for the proton of the isopropyl group. The two doublets centered at $\delta \approx 5.55$ and 5.38 correspond to the CH aromatic protons of the *p*-cymene rings. Complexes **13**–**14** exhibit a strong peak at $\delta = 2.25$ for the methyl protons of hexamethylbenzene ligand. In similar case with the Cp* analogues the arene ruthenium complexes also the chemical shifts of the arene ligands of ruthenium does not shifted down filed as compared to other N-based ligands, this could be due to the geometrical orientation of arene ligands to the benzene-linker [24–27].

*3.5. Crystal structure analysis of $[\{(\eta^5\text{-}C_5Me_5)IrCl\}_2(\mu\text{-}L1)]^{2+}$ ([**7**](PF$_6$)$_2$), $[\{(\eta^6\text{-}C_6H_6)RuCl\}_2(\mu\text{-}L1)]^{2+}$ ([**9**](PF$_6$)$_2$) and $[\{(\eta^6\text{-}p\text{-}^iPrC_6H_4Me)RuCl\}_2(\mu\text{-}L1)]^{2+}$ ([**11**](PF$_6$)$_2$)*

The molecular structure of complexes $[\{(\eta^5\text{-}C_5Me_5)IrCl\}_2(\mu\text{-}L1)]^{2+}$ ([**7**](PF$_6$)$_2$), $[\{(\eta^6\text{-}C_6H_6)RuCl\}_2(\mu\text{-}L1)]^{2+}$ ([**9**](PF$_6$)$_2$) and $[\{(\eta^6\text{-}p\text{-}^iPrC_6H_4Me)RuCl\}_2(\mu\text{-}L1)]^{2+}$ ([**11**](PF$_6$)$_2$) were determined by single crystal X-ray diffraction analysis. The crystallographic data are gathered in Table 1 and the selected bond lengths and angles for complexes [**7**](PF$_6$)$_2$, [**9**](PF$_6$)$_2$ and [**11**](PF$_6$)$_2$ are presented in Table 2. The corresponding ORTEP drawings are shown in Figs. 1, 2 and 3, respectively. All complexes show typical piano-stool geometry and have a half-sandwich structure consisting

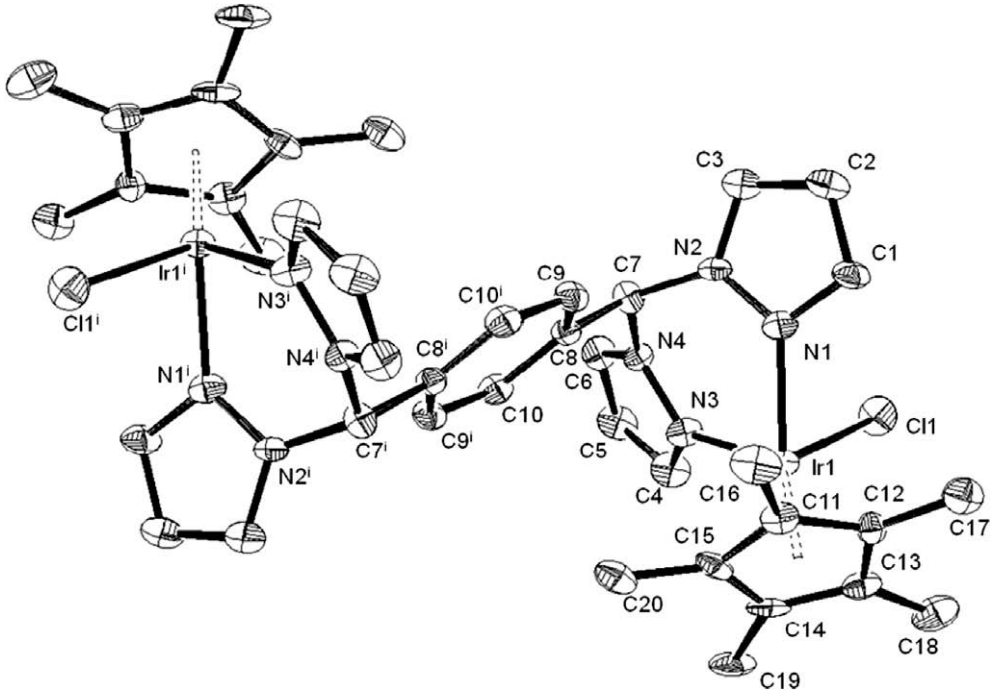

Fig. 1. ORTEP diagram with labelling scheme for [**7**](PF$_6$)$_2$·2CH$_3$CN, at 50% probability level, PF$_6$ anions and acetonitrile molecules omitted for clarity (symmetry code: i = 2 − *x*, 2 − *y*, −*z*).

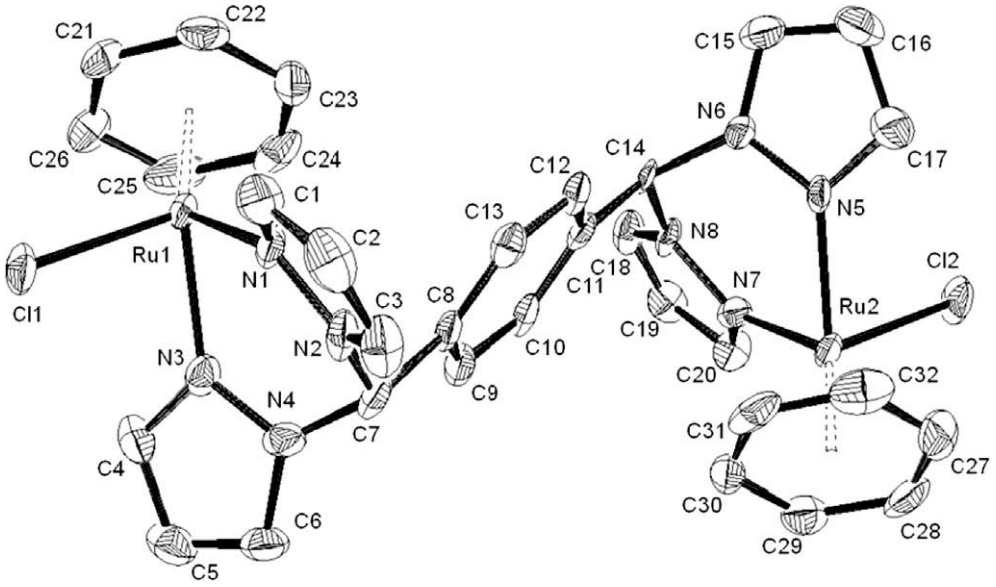

Fig. 2. ORTEP diagram with labelling scheme for [**9**](PF$_6$)$_2$·CH$_3$CN, at 50% probability level, PF$_6$ anions and acetonitrile molecules omitted for clarity.

of coordinated pentamethylcyclopentadienyl or arene; a chloride and the ligand through nitrogen's (see Figs. 1–3).

The distance of the iridium atoms and the corresponding centroids of η^5-C_5Me_5 rings is 1.79 Å in complex **7**. The distance between the ruthenium atoms and the centroid of the C_6H_6 and η^6-*p*-^{i}PrC$_6$H$_4$Me rings in complexes **9** and **11** are almost equivalent at 1.67 Å. These distances are comparable to those in the related complex cations [(η^6-*p*-^{i}PrC$_6$H$_4$Me)Ru(2-acetylthiazoleazine)Cl]$^+$ and [{(η^6-*p*-Pr^{i}C$_6$H$_4$Me)RuCl}$_2$(4,6-bis(3,5-dimethylpyrazolyl)-pyrimidine)]$^{2+}$ [24,40]. The average Ir–C distances of complex **7** is slightly shorter (2.16 Å) than the corresponding Ru–C distances. Indeed the average Ru–C distances of complex **9** are slightly shorter (2.17 Å) than the complex **11**, which is containing *p*-cymene ligand (2.19 Å). Which are almost identical to those reported iridium or rhodium complexes such as [(η^5-C_5Me_5)IrCl((S)-1-phenylethylsalicylaldiimine)] [2.17 Å] [41] and [(η^6-*p*-^{i}PrC$_6$H$_4$-Me)Ru(2-(2-thiazolyl)-1,8-naphthyridine)Cl]PF_6 [2.19 Å] [26].

The Ir–N bond distances of complex **7** at 2.110(6) and 2.093(6) Å are slightly longer than the Ru–N bond distances of complex **9** which are ranging from 2.081(4) to 2.089(5) Å, but are comparable to those found in **11** [2.102(4) and 2.098(4) Å]. All metal-chlorido bond distances are comparable, ranging from 2.391(1) to 2.395(2) Å, and are almost identical to other reported values [24,26]. In all complexes the η^5-C_5Me_5, η^6-C_6H_6 or η^6-*p*-^{i}PrC$_6$H$_4$Me rings are positioned opposite to each other to the benzene-linker and chlorine atoms of the two metal atoms are located at the periphery of the complexes. The N1–Ir1–N3 bond angle in complex **7** is found to be 86.0(2)° and in complexes **9** and **11** are found to be 84.3(2)°, 83.8(2)° and 85.1(2)°, respectively. These bond angles are comparable to those in the related complex cations [(η^6-C_6H_6)Ru(bpzmArOCH$_3$)]BPh_4 and [(η^6-*p*-^{i}PrC$_6$H$_4$Me)Ru-(bpzmArNO$_2$]BPh_4 [13].

All compounds crystallise with acetonitrile molecules, which surprisingly interact strongly with neither the cation nor the anions. However, all hydrogen atoms of the tertiary carbons (C7 as well as C14 in **9**) are involved in C–H···F or C–H···Cl interactions in the crystal packing. In [**7**]$(PF_6)_2$·2CH$_3$CN and [**11**]$(PF_6)_2$·2CH$_3$CN, the C···F separations are ranging from 3.31 to

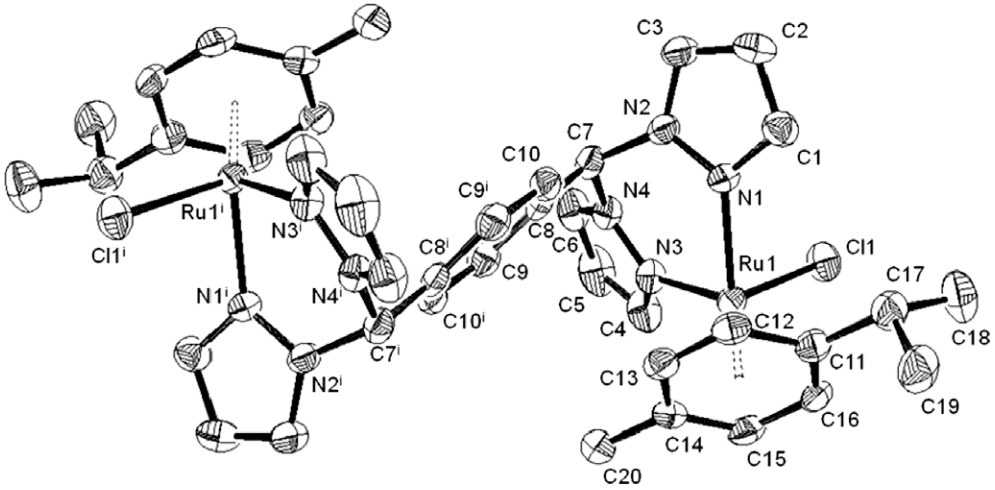

Fig. 3. ORTEP diagram with labelling scheme for [**11**]$(PF_6)_2$·2CH$_3$CN, at 50% probability level, PF_6 anions and acetonitrile molecules omitted for clarity (symmetry code: i = $-x$, $1-y$, $-z$).

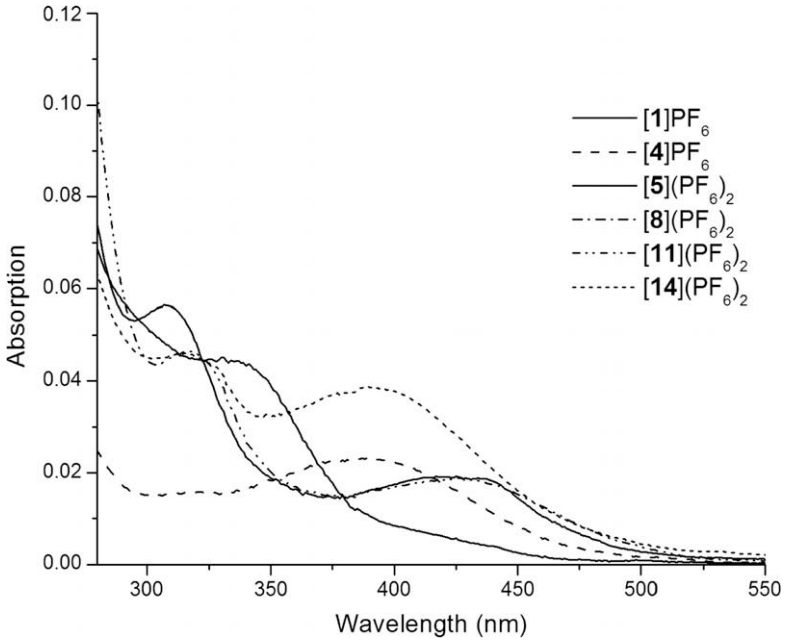

Fig. 4. UV–Vis electronic spectra of selected complexes (acetonitrile, 10^{-5} M, 298 K).

3.58 Å with C–H···F angles ranging from 131.3 to 163.1°, while in [**9**]$(PF_6)_2 \cdot CH_3CN$, the C···Cl distances are 3.40 and 3.43 Å with C–H···Cl angles of 153.2° and 142.8°, respectively.

3.6. UV–Vis spectroscopy

Electronic absorption spectra of the mononuclear compounds [**1**]PF_6–[**4**]PF_6 as well as the dinuclear compounds [**5**]$(PF_6)_2$–[**14**]$(PF_6)_2$ were acquired in acetonitrile, at 10^{-5} M concentration in the range 200–600 nm. Electronic spectra of representative complexes are depicted in Fig. 4 without showing the strong absorption at 224–229 nm. The spectra of these complexes are characterized by two main features, *viz*., an intense ligand-localized or intra-ligand $\pi \rightarrow \pi^*$ transition in the ultraviolet region and metal-to-ligand charge transfer (MLCT) $d\pi(M) \rightarrow \pi^*$ (L1 – ligand) bands in the visible region [42]. Since the low spin d^6 configuration of the mononuclear complexes provides filled orbitals of suitable symmetry at the Ru(II), Rh(III) and Ir(III) centers, these can interact with low lying π^* orbitals of the ligands. All mononuclear compounds [**1**]PF_6–[**4**]PF_6 show a high intensity band in the region 224–230 nm and a medium intensity band in the region 341–394 nm in UV region, these two bands are attributed to the ligand–localized or intra-ligand $\pi \rightarrow \pi^*$ transitions. Whereas the dinuclear complexes [**5**]$(PF_6)_2$–[**14**]$(PF_6)_2$ show three bands, for instance a high intensity band in the region 224–230 nm, a medium intensity band in the region 307–317 nm and a second medium intensity low energy absorption band in the visible region 394–437 nm. The medium intensity bands in the UV region is assigned to π–π^*, the high intensity band in the UV region is assigned to inter and intra-ligand π–π^*/n–π^* transitions [24,27], while the low energy absorption band in the visible region is assigned to metal-to-ligand charge transfer (MLCT) (t_{2g}–π^*).

5. Conclusions

In this work, we have showed that ligand L reacts with arene ruthenium and pentamethylcyclopentadienyl rhodium and iridium complexes to yield a series of mono and dinuclear complexes in good yield, which are remarkably stable in air as well as in solution. The Cp* rhodium and iridium derivatives yielded both mono and dinuclear complexes, while only dinuclear complexes are obtained with the arene ruthenium analogues, despite different molar ratio of ligands. In all these, both mono and dinuclear complexes the metal atom is bonded to the coordinated sites N1 and N3 or N4 and N6.

Acknowledgements

K.M. Rao gratefully acknowledges the Department of Science and Technology, New Delhi, (Sanction Order No. SR/S1/IC-11/2004) for financial support.

Appendix A. Supplementary Material

CCDC <757062>, <757063> and <757064> contains the supplementary crystallographic data for this paper. These data can be obtained free of charge from The Cambridge Crystallographic Data Centre via www.ccdc.cam.ac.uk/data_request/cif. Supplementary data associated with this article can be found, in the online version, at doi:10.1016/j.jorganchem.2010.02.005.

References

[1] S. Trofimenko, Scorpionates: The Coordination Chemistry of Polypyrazolylborate Ligands, Imperial College, London, 1999.
[2] S. Trofimenko, Chem. Rev. 93 (1993) 943–980.
[3] C. Pettinari, C. Santini, Compr. Coord. Chem. II 1 (2004) 159–210.
[4] D.L. Reger, Comments Inorg. Chem. 21 (1999) 1–28.
[5] H.R. Bigmore, S.C. Lawrence, P. Mountford, C.S. Tredget, J. Chem. Soc., Dalton Trans. (2005) 635–651.
[6] G.J. Long, F. Grandjean, D.L. Reger, Top. Curr. Chem. 233 (2004) 91–122.
[7] C. Pettinari, R. Pettinari, Coord. Chem. Rev. 249 (2005) 525–543.
[8] C. Pettinari, R. Pettinari, Coord. Chem. Rev. 249 (2005) 663.
[9] D.L. Reger, T.C. Grattan, K.J. Brown, C.A. Little, J.J.S. Lamba, L. Rheingold, R.D. Sommer, J. Organomet. Chem. 607 (2000) 120–128.
[10] S. Juliá, Org. Prep. Proced. Int. 16 (1984) 299–307.
[11] D.L. Reger, R.P. Watson, M.D. Smith, P.J. Pellechia, Organometallics 25 (2006) 743–755. and references therein.
[12] D. L. Reger, E. A. Foley, M. D. Smith, Inorg. Chem. doi:10.1021/ic901899r.
[13] M.C. Carrión, F. Sepúlveda, F.A. Jalón, B.R. Manzano, Organometallics 28 (2009) 3822–3833. and references therein.
[14] C. Slugovc, I. Padilla-Martínez, S. Sirol, E. Carmona, Coord. Chem. Rev. 213 (2001) 129–157.
[15] L.D. Field, B.A. Messerle, M. Rehr, L.P. Soler, T.W. Hambley, Organometallics 22 (2003) 2387–2395.
[16] E. Teuma, M. Loy, C. Le Berre, M. Etienne, J.-C. Daran, P. Kalck, Organometallics 22 (2003) 5261–5267.
[17] S. Burling, L.D. Field, B.A. Messerle, S.L. Rumble, Organometallics 26 (2007) 4335–4343.
[18] A.W. Stumpf, E. Saive, A. Demonceau, A.F. Noels, J. Chem. Soc., Chem. Commun. (1995) 1127–1128.
[19] B. Therrien, G. Süss-Fink, P. Govindaswamy, A.K. Renfrew, P.J. Dyson, Angew. Chem., Int. Ed. 47 (2008) 3773–3776.
[20] Y.-K. Yan, M. Melchart, A. Habtemariam, P.J. Sadler, Chem. Commun. (2005) 4764–4776. and references therein.
[21] K.S. Singh, Y.A. Mozharivskyj, K. Mohan Rao, Z. Anorg. Allg. Chem. 632 (2005) 172–179.
[22] P. Govindaswamy, P.J. Carroll, Y.A. Mozharivskyj, K. Mohan Rao, J. Organomet. Chem. 690 (2005) 885–894.
[23] G. Gupta, G.P.A. Yap, B. Therrien, K. Mohan Rao, Polyhedron 28 (2009) 844–850.
[24] K.T. Prasad, B. Therrien, S. Geib, K. Mohan Rao, J. Organomet. Chem. 696 (2010) 495–504.
[25] G. Gupta, K.T. Prasad, B. Das, G.P.A. Yap, K. Mohan Rao, J. Organomet. Chem. 694 (2009) 2618–2627.
[26] K.T. Prasad, B. Therrien, K.M. Rao, J. Organomet. Chem. 693 (2008) 3049–3056.
[27] K.T. Prasad, B. Therrien, K.M. Rao, J. Organomet. Chem. (2009) 695 (2010) 226–234.
[28] E.A. Nudnova, A.S. Potapov, A.I. Khlebnikov, V.D. Ogorodnikov, Russ. J. Org. Chem. 43 (2007) 1698–1702.
[29] M.A. Bennett, T.N. Huang, T.W. Matheson, A.K. Smith, Inorg. Synth. 21 (1982) 74–78.
[30] M.A. Bennett, T.W. Matheson, G.B. Robertson, A.K. Smith, P.A. Tucker, Inorg. Chem. 19 (1980) 1014–1021.
[31] M.A. Bennett, A.K. Smith, J. Chem. Soc., Dalton Trans. (1974) 233–241.
[32] J.W. Kang, K. Moseley, P.M. Maitlis, J. Am. Chem. Soc. 91 (1969) 5970–5977.
[33] R.G. Ball, W.A.G. Graham, D.M. Heinekey, J.K. Hoyano, A.D. McMaster, B.M. Mattson, S.T. Michel, Inorg. Chem. 29 (1990) 2023–2025.
[34] C. White, A. Yates, P.M. Maitlis, Inorg. Synth. 29 (1992) 228.
[35] G.M. Sheldrick, Acta Crystallogr., Sect. A 46 (1990) 467–473.
[36] G.M. Sheldrick, SHELXS-97 and SHELXL-97, University of Göttingen, Göttingen, Germany, 1999.
[37] L.J. Farrugia, J. Appl. Crystallogr. 30 (1997) 565–566.
[38] A.S. Potapov, G.A. Domina, A.I. Khlebnikov, V.D. Ogorodnikov, Eur. J. Org. Chem. (2007) 5112.
[39] H. Van der Poel, G. Van Koten, K. Vrieze, Inorg. Chem. 19 (1980) 1145–1151.
[40] K.T. Prasad, G. Gupta, A.V. Rao, B. Das, K. Mohan Rao, Polyhedron 28 (2009) 2649–2654.
[41] H. Brunner, A. Köllnberger, T. Burgemeister, M. Zabel, Polyhedron 19 (2000) 1519–1526.
[42] E. Binamira-Soriaga, N.L. Keder, W.C. Kaska, Inorg. Chem. 29 (1990) 3167–3171.